Hole Transport | Hot Paper

A Simple 3,4-Ethylenedioxythiophene Based Hole-Transporting Material for Perovskite Solar Cells**

Hairong Li, Kunwu Fu, Anders Hagfeldt, Michael Grätzel, Subodh G. Mhaisalkar,* and Andrew C. Grimsdale*

Abstract: *We report a novel electron-rich molecule based on 3,4-ethylenedioxythiophene (H101). When used as the hole-transporting layer in a perovskite-based solar cell, the power-conversion efficiency reached 13.8% under AM 1.5G solar simulation. This result is comparable with that obtained using the well-known hole transporting material 2,2′,7,7′-tetra-kis(N,N-di-p-methoxyphenylamine)-9,9′-spirobifluorene (spiro-OMeTAD). This is the first heterocycle-containing material achieving >10% efficiency in such devices, and has great potential to replace the expensive spiro-OMeTAD given its much simpler and cheaper synthesis.*

Undoubtedly, in order to get dye-sensitized solar cells (DSSC) into the commercial market, the all-solid-state DSSC is an attractive design choice. As a result, research groups are making great efforts to optimize hole-transporting materials (HTMs) for such devices as an alternative to liquid electrolyte-based cells. Although inorganic HTMs such as the recently developed $CsSnI_3$[1] are gaining serious attention, to date 2,2′,7,7′-tetrakis(N,N-di-p-methoxyphenylamine)-9,9′-spirobifluorene (spiro-OMeTAD; Figure 1) is the main, indeed almost the only, organic HTM being extensively studied[2] Much device optimization work, including doping, pore-filling, thickness and porosity of TiO_2, and reduction of recombination, is centered on spiro-OMeTAD, with the aid of sophisticated photophysical characterization and theoretical calculations. Compared with conventional DSSC materials, perovskites are a new generation of low cost inorganic nanocrystalline sensitizers showing excellent (>13%) power-conversion efficiency (PCE, η), which have rapidly become the hottest topic in DSSC research since late 2011.[2z,3]
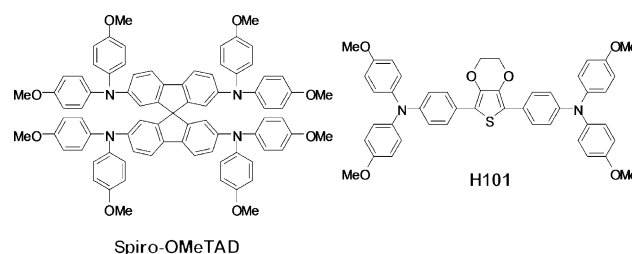

Figure 1. Chemical structures of spiro-OMeTAD and H101.

Although spiro-OMeTAD continues to be the best performing candidate HTM, several small molecules,[4] as well as classical polymers used extensively in organic photovoltaic devices (OPV), have also been investigated recently, including P3HT ($\eta = 6.7\%$), PCPDTBT ($\eta = 5.3\%$), PCDTBT ($\eta = 4.2\%$) and PTAA (typically $\eta = 9.0\%$, best 12.0%).[3b] It can be seen that only PTAA shows comparable PCE to spiro-OMeTAD; the other HTMs reported thus far display inferior performance for as yet unknown reasons. It is also reported that the semiconducting TiO_2 can be replaced by cheaper materials such as insulating Al_2O_3, acting as a scaffold without necessarily participating in the charge transport process;[5] thus, the highest cost of materials in DSSCs is now that of spiro-OMeTAD, which is very expensive because of its multistep synthesis. Therefore it is imperative, from a commercialization viewpoint, to develop efficient, yet cost-effective HTMs.

We herein report a new hole-transporting molecule 2,5-bis(4,4′-bis(methoxyphenyl)aminophen-4″-yl)-3,4-ethylene-dioxythiophene (H101; Figure 1). As shown in Scheme 1, the synthesis of H101 is much shorter than that of spiro-OMeTAD. 3,4-ethylenedioxythiophene was brominated in freshly distilled THF at room temperature followed by the addition of degassed base solution, a Pd catalyst, and 4[6] to perform a Suzuki coupling in the same pot. This one-pot two-

[*] Dr. H. Li,[+] K. Fu,[+] Prof. S. G. Mhaisalkar, Prof. A. C. Grimsdale
Energy Research Institute @ NTU (ERI@N), School of Materials Science and Engineering, Nanyang Technological University
Nanyang Avenue, Singapore 637553 (Singapore)
E-mail: Subodh@ntu.edu.sg
acgrimsdale@ntu.edu.sg

Prof. A. Hagfeldt
Department of Chemistry—Ångström Uppsala University
Box 523, 75120 Uppsala (Sweden)

Prof. M. Grätzel
Laboratory for Photonics and Interfaces, Institute of Chemical Sciences and Engineering, School of Basic Sciences, Ecole Poly-technique Fédérale de Lausanne, 1015 Lausanne (Switzerland)
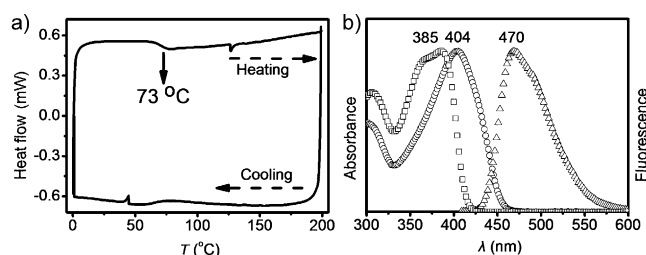
[+] These authors contributed equally to this work.
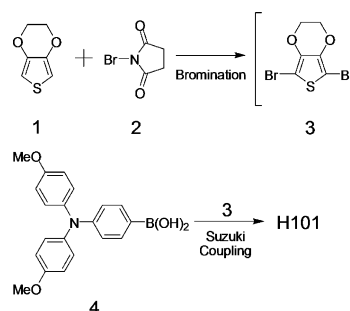
Scheme 1. Synthetic route to H101.

Figure 2. a) Differential scanning calorimetry of H101, with glass transition at 73 °C. b) Absorption (○) and emission (△) spectra of H101, and absorption (□) spectrum of spiro-OMeTAD.

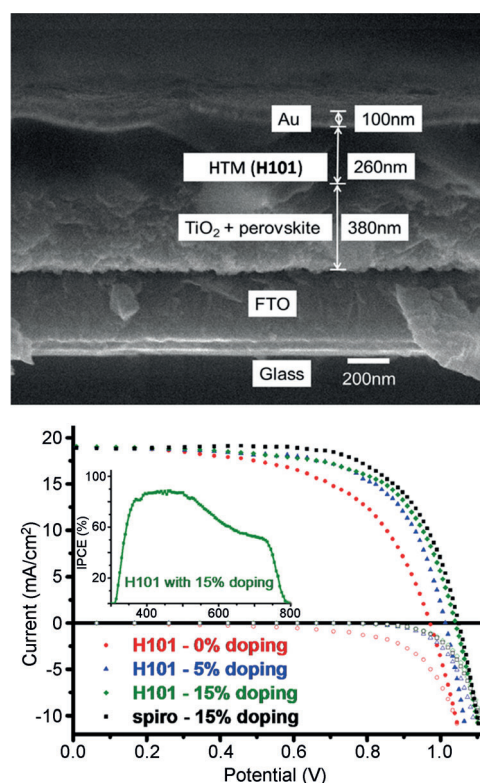step process gave an excellent overall yield of 82%, without optimization.

Differential scanning calorimetry (DSC) measurements show that H101 has a much lower (around 73 °C) glass transition temperature (T_g) than spiro-OMeTAD ($T_g = 125$ °C; Figure 2 a).[7] Absorption spectra (Figure 2 b) indicate that H101 starts to absorb light from 460 nm, and the absorption peak maximum is at 404 nm; this is ca. 20 nm red-shifted compared with the maxima for spiro-OMeTAD. The fluorescence spectrum of H101 shows a maximum at 470 nm with a large Stokes shift of 66 nm, which implies that it can undergo large geometrical changes upon excitation. We anticipated that the large Stokes shift, lower T_g, and smaller molecule size versus spiro-OMeTAD would be synergistically beneficial in the infiltration and pore-filling of a hole-transporting material by simple annealing or light soaking post-treatment. Cyclic voltammetry (CV) measurements indicate that the highest occupied molecular orbital (HOMO) level of H101 is around −5.16 eV, which is 50 mV higher than that of spiro-OMeTAD (−5.21 eV; Figure 3). In principle, the open-circuit voltage (V_{oc}) of a conventional solid-state dye-sensitized solar cell is determined by the difference between the quasi-Fermi levels of the electrons in the TiO_2 and the holes in the HTM.[8] From the electrochemical experiment one would expect that the V_{oc} from devices with H101 as a hole-transporting material would be slightly lower than that from devices using spiro-OMeTAD. In addition, chemical doping is commonly used to further lower the Fermi level of the HTM and increase its conductivity, thus improving device performance.[9] It can be observed from the absorbance spectra that as the doping level of the cobalt dopant tris(2-(1*H*-pyrazol-1-yl)pyridine)cobalt(III) (FK102)[2j] increases, the absorbance feature of the oxidized H101 species gradually increases in the visible range from 500–700 nm (Figure 3). This demonstrates
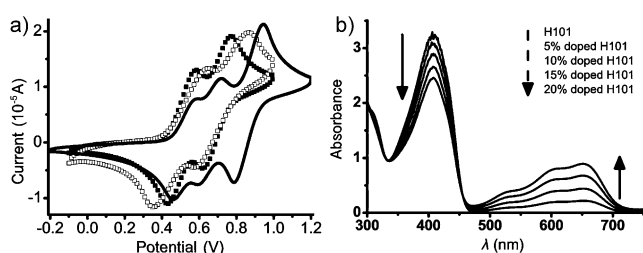
the effective chemical doping of H101 by the FK102, which is expected to improve the V_{oc} by lowering the HOMO level, and improve the fill factor by improving the charge-transport properties.

A scanning electron microscope (SEM) image of the device cross-section shows the typical structural configuration of a perovskite solar cell (Figure 4). It can be seen that a 380 nm thick mesoporous TiO_2 film, loaded with $CH_3NH_3PbI_3$ perovskite as a sensitizer, is sandwiched between a conductive fluorine-doped tin oxide (FTO) substrate and a 260 nm thick hole-transporting layer (H101), with an evaporated 100 nm thick gold layer as the cathode. In this configuration, under illumination, perovskite absorbs the incident light and generates charge carriers where electrons are injected into the TiO_2 conduction band and from there into the FTO, while the corresponding holes are conducted through the hole-transporting layer to the cathode.[10] Under 1 Sun illumination, the devices with H101 as a hole-transporting layer achieved a PCE of 10.6% without doping, whereas the fully optimized reference device, based on spiro-OMeTAD with 15% FK102 doping, attained an efficiency of 13.7% in a parallel experiment (Table 1). It was clear that the device with H101 had a current density (J_{sc}) as high as that of spiro-OMeTAD, wherein the EDOT is thought to play an important role. Our initial screening of other HTM candidate materials revealed that replacing the EDOT core with unsubstituted benzene or thiophene resulted in a much lower current. The open circuit voltage (V_{oc}) of the device with the undoped H101 is 0.97 V, which was lower than that of

Figure 3. a) CV spectra of spiro-OMeTAD and H101. b) Absorption spectra of H101 with different doping ratios in chlorobenzene.

Figure 4. Cross-sectional SEM picture of a typical perovskite solar-cell device and current–voltage curves of solar cells based on spiro-OMeTAD and H101 as HTM. Inset shows the IPCE spectra of the perovskite solar cell with 15% doped H101 as HTM.

⇖⇖ These are not the final page numbers!

Table 1: I–V characteristics of photovoltaic measurements.

HTM[a]	PCE [%]	J_{sc} [mA cm^{-2}]	V_{oc} [V]	FF	R_s
H101 (0)	10.6 ± 0.53	18.9 ± 1.21	0.97 ± 0.02	0.57 ± 0.02	29.6
H101 (5)	12.6 ± 0.28	19.0 ± 0.61	1.02 ± 0.01	0.64 ± 0.03	18.4
H101 (15)	13.2 ± 0.57 (13.8)	19.1 ± 1.05 (20.5)	1.05 ± 0.02 (1.04)	0.65 ± 0.03 (0.65)	14.6
spiro[b] (15)	13.7	18.9	1.05	0.69	–

[a] Doping percentage is given in parentheses. [b] spiro = spiro-OMeTAD.

spiro-OMeTAD (1.05 V), as expected due to the relatively higher HOMO level of H101. However, the effect of chemical doping by FK102 was validated by varying the doping concentration. An enhancement of V_{oc} was observed, as shown in Figure 4 and summarized in Table 1. It was shown that the chemical doping of H101 by FK102 could lower the Fermi level of H101 to generate higher voltage in the devices, from 0.97 V for an undoped cell to 1.05 V with 15% doping. The CV spectra in Figure 3 also indicated that the two characteristic oxidation peaks of H101 shifted to higher potential with 15% doping as compared to those of the undoped one; moreover, the increased hole conductivity after doping also helped increase the fill factor (FF) from 0.57 with pristine H101 to 0.65 with 15% doping, which was supported by the constantly decreasing value of the series resistance (R_s; estimated from a solar simulator; Table 1). As a result, the PCE of the H101-based solar cell reached an average of 13.2% (maximum of 13.8%). To the best of our knowledge, this is the first reported thiophene-based HTM to show a high (>10%) efficiency in perovskite solar cells. Indeed, its overall performance was comparable with the best results obtained using spiro-OMeTAD (PCE = 13.7%; Table 1) in our laboratory.

For the stability test, we accelerated the aging by putting the cells in an oven at 70 °C for 7 days and measured the I–V response each day. The photovoltaic data are summarized in the Figure 5. The results show that both spiro-OMeTAD and H101 have comparable thermal stability. The moderate decreases in performance (ca. 15%) for both spiro-OMeTAD- and H101-based devices are within expectation for unpackaged cells. It is clear that the open-circuit voltage of both samples showed only a slight decrease, whereas the short-circuit current and fill factor were the main parameters affected, which is primarily attributed to the moisture-

induced degradation of the very hygroscopic perovskite. The results also showed that the low glass transition temperature of H101 did not induce the durability issue.

In conclusion, we have reported H101, a new simple HTM incorporating a readily available EDOT unit as the core structure, and obtained PCE comparable with devices using spiro-OMeTAD. These results have shown that it is possible to introduce suitable heterocyclic structures into the HTM design to achieve high performance, yet with much simpler chemistry and much lower production cost. Furthermore, it leads to possibilities for modification of the chemical structure without restrictions to phenylamine derivatives. Thus, it becomes easier and more accessible to increase the mobility and tune the band gap. Through chemical doping of H101 with FK102, device performance was further improved with enhanced V_{oc} owing to the shift in the hole Fermi level, making H101 an excellent candidate to replace spiro-OMeTAD. Thus far, we have followed standard methods for device fabrication, without optimizing specifically for H101. Further increase in performance appears feasible by modifying the chemical structures and fine-tuning the device parameters. An important aspect for HTMs is the ability of the material to be processed in cell and module manufacturing. For H101 and derivatives, we envisage large-scale production methods, such as melting and printing techniques.

Experimental Section

Synthesis of 2,5-bis(4,4′-bis(methoxyphenyl)aminophen-4″-yl)-3,4-ethylenedioxythiophene (H101). Compound **1** (0.3 g, 2.11 mmol) and *N*-bromosuccinimide (NBS; 0.75 g, 4.22 mmol) were dissolved in freshly distilled THF (20 mL) and stirred at RT for 2 h under N$_2$. The reaction solution was transferred by syringe into a N$_2$-protected 50 mL flask containing K$_2$CO$_3$ (2 M, 5 mL), Pd^0(PPh$_3$)$_4$ (0.12 g, 0.1 mmol), and **4** (1.47 g, 4.22 mmol). The reaction mixture was then stirred at reflux in the dark for 6 h. The reaction mixture was cooled to RT and poured into water, extracted with CH$_2$Cl$_2$, and washed with water. The CH$_2$Cl$_2$ layer was dried over MgSO$_4$ and concentrated, and the residue was purified by column chromatography on silica gel, eluting with CH$_2$Cl$_2$ to obtain the product as a yellow solid (1.3 g, 82%). ^{1}H NMR (CD$_2$Cl$_2$): δ = 7.55 (br, 4H), 7.07 (d, J = 8.4 Hz, 8H), 6.90 (d, J = 7.6 Hz, 4H), 6.86 (d, J = 8.8 Hz, 8H), 4.34 (s, 4H), 3.81 ppm (s, 12H). ^{13}C NMR (CD$_2$Cl$_2$): δ = 156.5, 147.7, 141.1, 138.3, 127.0, 125.8, 120.9, 115.1, 65.1, 55.9 ppm. HRMS (MALDI-TOF): calcd for C$_{46}$H$_{40}$N$_2$O$_6$S, 748.2607; found, 748.2656. Anal. calcd. for C$_{46}$H$_{40}$N$_2$O$_6$S: C, 73.78; H, 5.38; N, 3.74; S, 4.28%. Found: C, 74.01; H, 5.29; N, 3.70; S, 4.21%.

Device fabrication. FTO glass was etched with Zinc powder and aqueous HCl (2 M). A compact layer of TiO$_2$ was deposited onto the FTO surface by a spray pyrolysis process using titanium diisopropoxide bis(acetylacetonate) solution (75% in isopropyl alcohol (IPA); Sigma–Aldrich) diluted in ethanol (1:9 v/v). After cooling to room temperature, the substrates were treated in a TiCl$_4$ solution (0.04 M) for 30 min at 70 °C. A mesoporous TiO$_2$ film was spin-coated onto the FTO surface using 30 nm TiO$_2$ nanoparticle paste diluted with ethanol (1:5 w/w) and sintered at 500 °C for 30 min. The films were treated with a TiCl$_4$ solution (40 mM) at 70 °C for 30 min and heated at 500 °C, again for 30 min. After cooling to RT, PbI$_2$ solution (1 M) was spin-coated onto the mesoporous film, which was then heated at 70 °C
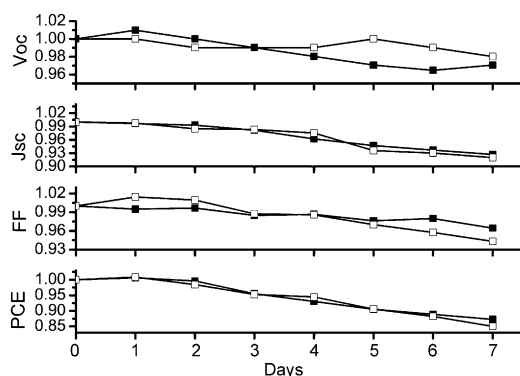
Figure 5. Thermal aging test for devices based on H101 (□) and spiro-OMeTAD (■).

for 30 min. The films were then immersed into a solution of CH_3NH_3I in IPA (8 mg mL^{-1}) for 15 min, after which they were rinsed with IPA and dried by spinning at 4000 rpm for 30 s, followed by annealing at 70 °C for 30 min. Spiro-OMeTAD (for the reference cell) and H101 were each dissolved in chlorobenzene (100 mg mL^{-1}), with heating to 70 °C for 30 min. *tert*-butylpyridine (TBP; 15.92 μL) and lithium bis(trifluoromethylsulfonyl)imide (Li-TFSI, 9.68 μL, 520 mg mL^{-1} in acetonitrile) were added directly to aliquots (300 μL) of the HTM solutions. Co-dopant tris(2-(1*H*-pyrazol-1-yl)pyridine)cobalt(III) tris(hexafluorophosphate) (FK102) was predissolved into acetonitrile and added into the hole-transport-material solution at ratios of 5–15 mol %. The as-prepared solutions were spin-coated onto the film at 4000 rpm for 30 s. A 100 nm Au cathode layer was deposited by thermal evaporation through a 0.2 cm^2 metallic mask.

Equipment. ^{1}H and ^{13}C NMR data were obtained on a Bruker DPX 400 MHz spectrometer with chemical shifts referenced to CD_2Cl_2. Cyclic voltammetry measurements were carried out on a CHI411 electrochemical workstation, using a concentration of a few mM in dichloromethane containing tetrabutylammoniun hexafluorophosphate, $Bu_4N^+PF_6^-$ (ca. 0.05 M; as a supporting electrolyte) in a three-electrode cell, where the Ag/AgCl electrode was used as the reference electrode and platinum wire as the working electrode. The scanning rate was 100 mV s^{-1}. The absorption spectra of the chemically doped H101 were measured using a UV/Vis spectrometer (SHIMADZU, UV-3600 UV/Vis/NIR Spectrophotometer). Fluorescence measurements were carried out on a RF-5301PC Shimadzu spectrofluorophotometer. Differential scanning calorimetry (DSC) was run on a TA Instrument Q10. Photovoltaic measurements utilized an AM 1.5G solar simulator equipped with a 450 W xenon lamp (model 81172, Oriel). Its power output was adjusted to match AM 1.5G sunlight (100 mW cm^{-2}) by using a reference Si photodiode. *I–V* curves were obtained by applying an external bias from 1.2 V to −0.05 V (reverse scan mode) to the cell and measuring the generated photocurrent with a Keithley model 2612A digital source meter. The total measuring points were 101 and the delay between measurement points was set at 0.1 second. All devices were measured by masking the active area with a black tape mask with an active area of 0.2 cm^2. Incident photon-to-current conversion efficiency (IPCE) was measured using a PVE300 (Bentham), with dual Xenon/quartz halogen light source, measured in DC mode, and no bias light was used. The cross-sectional view of the perovskite-based solar-cell devices was obtained with a field-emission scanning electron microscopy (FE-SEM, JOEL JSM 7600F).

[1] I. Chung, B. Lee, J. He, R. P. H. Chang, M. G. Kanatzidis, *Nature* **2012**, *485*, 486–489.

[2] a) L. Yang, U. B. Cappel, E. L. Unger, M. Karlsson, K. M. Karlsson, E. Gabrielsson, L. Sun, G. Boschloo, A. Hagfeldt, E. M. J. Johansson, *Phys. Chem. Chem. Phys.* **2012**, *14*, 779–789; b) C.-Y. Hsu, Y.-C. Chen, R. Y.-Y. Lin, K.-C. Ho, J. T. Lin, *Phys. Chem. Chem. Phys.* **2012**, *14*, 14099–14109; c) A. Dualeh, J. H. Delcamp, M. K. Nazeeruddin, M. Grätzel, *Appl. Phys. Lett.* **2012**, *100*, 173512–173514; d) O. Rana, R. Srivastava, R. Grover, M. Zulfequar, M. Husain, M. N. Kamalasanan, *Synth. Met.* **2011**, *161*, 828–832; e) C. Olson, D. Veldman, K. Bakker, F. Lenzmann, *Int. J. Photoenergy* **2011**, *2011*, 1–11; f) J. Melas-Kyriazi, I. K. Ding, A. Marchioro, A. Punzi, B. E. Hardin, G. F. Burkhard, N. Tétreault, M. Grätzel, J.-E. Moser, M. D. McGehee, *Adv. Energy Mater.* **2011**, *1*, 407–414; g) X. Jiang, K. M. Karlsson, E. Gabrielsson, E. M. J. Johansson, M. Quintana, M. Karlsson, L. Sun, G. Boschloo, A. Hagfeldt, *Adv. Funct. Mater.* **2011**, *21*, 2944–2952; h) S. Fantacci, F. De Angelis, M. K. Nazeeruddin, M. Grätzel, *J. Phys. Chem. C* **2011**, *115*, 23126–23133; i) N. Cai, S.-J. Moon, L. Cevey-Ha, T. Moehl, R. Humphry-Baker, P. Wang, S. M. Zakeeruddin, M. Grätzel, *Nano Lett.* **2011**, *11*, 1452–1456; j) see Ref. [9]; k) S.-J. Moon, Y. Itzhaik, J.-H. Yum, S. M. Zakeeruddin, G. Hodes, M. Grätzel, *J. Phys. Chem. Lett.* **2010**, *1*, 1524–1527; l) U. B. Cappel, E. A. Gibson, A. Hagfeldt, G. Boschloo, *J. Phys. Chem. C* **2009**, *113*, 6275–6281; m) H. J. Snaith, R. Humphry-Baker, P. Chen, I. Cesar, S. M. Zakeeruddin, M. Grätzel, *Nanotechnology* **2008**, *19*, 424003; n) H. J. Snaith, A. J. Moule, C. Klein, K. Meerholz, R. H. Friend, M. Grätzel, *Nano Lett.* **2007**, *7*, 3372–3376; o) H. J. Snaith, M. Grätzel, *Adv. Mater.* **2007**, *19*, 3643–3647; p) W. H. Howie, J. E. Harris, J. R. Jennings, L. M. Peter, *Sol. Energy Mater. Sol. Cells* **2007**, *91*, 424–426; q) H. J. Snaith, M. Grätzel, *Appl. Phys. Lett.* **2006**, *89*, 262114/1–262114/3; r) L. Schmidt-Mende, U. Bach, R. Humphry-Baker, T. Horiuchi, H. Miura, S. Ito, S. Uchida, M. Grätzel, *Adv. Mater.* **2005**, *17*, 813–815; s) J. Kirkpatrick, J. Nelson, *J. Chem. Phys.* **2005**, *123*, 084703; t) J. Krüger, R. Plass, M. Grätzel, P. J. Cameron, L. M. Peter, *J. Phys. Chem. B* **2003**, *107*, 7536–7539; u) J. Krüger, R. Plass, L. Cevey, M. Piccirelli, M. Grätzel, U. Bach, *Appl. Phys. Lett.* **2001**, *79*, 2085–2087; v) J. Krüger, U. Bach, M. Grätzel, *Adv. Mater.* **2000**, *12*, 447–451; w) U. Bach, Y. Tachibana, J.-E. Moser, S. A. Haque, J. R. Durrant, M. Grätzel, D. R. Klug, *J. Am. Chem. Soc.* **1999**, *121*, 7445–7446; x) U. Bach, D. Lupo, P. Comte, J. E. Moser, F. Weissortel, J. Salbeck, H. Spreitzer, M. Grätzel, *Nature* **1998**, *395*, 583–585; y) M. Liu, M. B. Johnston, H. J. Snaith, *Nature* **2013**, *501*, 395–398; z) M. M. Lee, J. Teuscher, T. Miyasaka, T. N. Murakami, H. J. Snaith, *Science* **2012**, *338*, 643–647; aa) J. H. Noh, N. J. Jeon, Y. C. Choi, M. K. Nazeeruddin, M. Gratzel, S. I. Seok, *J. Mater. Chem. A* **2013**, *1*, 11842–11847.

[3] a) J.-Y. Jeng, Y.-F. Chiang, M.-H. Lee, S.-R. Peng, T.-F. Guo, P. Chen, T.-C. Wen, *Adv. Mater.* **2013**, *25*, 3727–3732; b) J. H. Heo, S. H. Im, J. H. Noh, T. N. Mandal, C.-S. Lim, J. A. Chang, Y. H. Lee, H.-j. Kim, A. Sarkar, M. K. Nazeeruddin, M. Grätzel, S. I. Seok, *Nat. Photonics* **2013**, *7*, 486–491; c) M. J. Carnie, C. Charbonneau, M. L. Davies, J. Troughton, T. M. Watson, K. Wojciechowski, H. Snaith, D. A. Worsley, *Chem. Commun.* **2013**, *49*, 7893–7895; d) B. Cai, Y. Xing, Z. Yang, W.-H. Zhang, J. Qiu, *Energy Environ. Sci.* **2013**, *6*, 1480–1485; e) H.-S. Kim, C.-R. Lee, J.-H. Im, K.-B. Lee, T. Moehl, A. Marchioro, S.-J. Moon, R. Humphry-Baker, J.-H. Yum, J. E. Moser, M. Grätzel, N.-G. Park, *Sci. Rep.* **2012**, *2*, 591; f) L. Etgar, P. Gao, Z. Xue, Q. Peng, A. K. Chandiran, B. Liu, M. K. Nazeeruddin, M. Grätzel, *J. Am. Chem. Soc.* **2012**, *134*, 17396–17399; g) J.-H. Im, C.-R. Lee, J.-W. Lee, S.-W. Park, N.-G. Park, *Nanoscale* **2011**, *3*, 4088–4093.

[4] a) D. Bi, L. Yang, G. Boschloo, A. Hagfeldt, E. M. J. Johansson, *J. Phys. Chem. Lett.* **2013**, *4*, 1532–1536; b) E. Edri, S. Kirmayer, D. Cahen, G. Hodes, *J. Phys. Chem. Lett.* **2013**, *4*, 897–902.

[5] H. J. Snaith, *J. Phys. Chem. Lett.* **2013**, *4*, 3623–3630.

[6] For the synthesis of **4**, see: C. Teng, X. Yang, C. Yang, S. Li, M. Cheng, A. Hagfeldt, L. Sun, *J. Phys. Chem. C* **2010**, *114*, 9101–9110.

[7] T. Leijtens, I. K. Ding, T. Giovenzana, J. T. Bloking, M. D. McGehee, A. Sellinger, *ACS Nano* **2012**, *6*, 1455–1462.

[8] A. Hagfeldt, G. Boschloo, L. Sun, L. Kloo, H. Pettersson, *Chem. Rev.* **2010**, *110*, 6595–6663.

[9] J. Burschka, A. Dualeh, F. Kessler, E. Baranoff, N. L. Cevey-Ha, C. Yi, M. K. Nazeeruddin, M. Gratzel, *J. Am. Chem. Soc.* **2011**, *133*, 18042–18045.

[10] H. S. Kim, C. R. Lee, J. H. Im, K. B. Lee, T. Moehl, A. Marchioro, S. J. Moon, R. Humphry-Baker, J. H. Yum, J. E. Moser, M. Grätzel, N. G. Park, *Sci. Rep.* **2012**, *2*, 591.
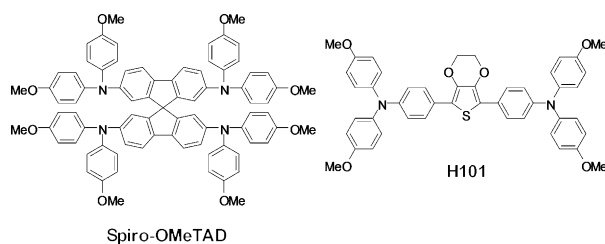
Angew. Chem. Int. Ed. **2014**, *53*, 1–5

◤◤ These are not the final page numbers!

Communications

Hole Transport

H. Li, K. Fu, A. Hagfeldt, M. Grätzel,
S. G. Mhaisalkar,*
A. C. Grimsdale* —————— ▪▪▪▪–▪▪▪▪

A Simple 3,4-Ethylenedioxythiophene
Based Hole-Transporting Material for
Perovskite Solar Cells

Spiro-OMeTAD   H101

Heterocycle power! A power-conversion efficiency of 13.8% under AM 1.5G illumination was achieved in a perovskite-based solar cell with a new hole-transporting material based on 3,4-ethylene-dioxythiophene (H101). This is the first heterocycle-containing material with >10% efficiency in such devices, and has great potential to replace the more expensive spiro-OMeTAD, given its much simpler and less expensive synthesis.